

# Design and Evaluation of Finite and Small Antennas at 0.97 GHz for Lightning Remote Sensing

B. Y. Seah<sup>1</sup>, M. R. Ahmad<sup>1\*</sup>, A. A. AlKahtani<sup>2</sup>, M. R. M. Esa<sup>3</sup>, M. A. B. Sidik<sup>4</sup>, S. A. S. Baharin<sup>1</sup>, M. H. M. Sabri<sup>2</sup>, N. Yusop<sup>5</sup>, M. Z. A. A. Aziz<sup>1</sup>, A. S. Al-Khaleefa<sup>1</sup>, N. A. Shairi<sup>1</sup> and M. Z. A. AB. Kadir<sup>2</sup>

<sup>1</sup>Atmospheric and Lightning Research Laboratory (ThorLab), Centre for Telecommunication Research and Innovation (CeTRI), Fakulti Kejuruteraan Elektronik dan Kejuruteraan Komputer (FKEKK), Universiti Teknikal Malaysia Melaka, Jalan Hang Tuah Jaya, 76100 Durian Tunggal, Melaka, Malaysia.

<sup>2</sup>Universiti Tenaga Nasional, Jalan IKRAM-UNITEN, 43000 Kajang, Selangor, Malaysia

<sup>3</sup>Institut Voltan and Arus Tinggi (IVAT), School of Electrical Engineering, Faculty of Engineering, Universiti Teknologi Malaysia, 81310 UTM Skudai, Johor, Malaysia

<sup>4</sup>Department of Electrical Engineering, Universitas Sriwijaya (UNSRI), 30662, Sumatera Selatan, Indonesia

<sup>5</sup>Department of Space Science Centre (ANGKASA), Institute of Climate Change, Universiti Kebangsaan Malaysia, 43600, Bangi, Selangor Darul Hossen, Malaysia  
riduan@utem.edu.my; abubakar@unsri.ac.id

## Article Info

Volume 81

Page Number: 5654 - 5662

Publication Issue:

November-December 2019

## Abstract

This paper presents the analysis of the UHF signature associated with positive and negative narrow bipolar events (+NBEs and -NBEs) captured by using a finite antenna (the largest dimension comparable to the wavelength of the incident electric field) and a small antenna (the largest dimension less than one tenth of the wavelength of the incident electric field). Both antennas have been designed and simulated in Computer Simulation Technology (CST) simulator. The finite antenna was calibrated inside anechoic chamber and was found to have resonant frequency at 0.97 GHz with 20 MHz bandwidth and omnidirectional radiation pattern. Measurements have been conducted between November and December 2018 where 120 UHF samples and 69 UHF samples had been captured by small antenna and finite antenna, respectively, together with their corresponding low frequency records (lower than 1 MHz), also known as fast antenna record (FA record). In average, the UHF peak amplitudes of the finite antenna are 22% larger than the small antenna and the former has better SNR which would ease the characterization of the UHF signals.

**Keywords:** Lightning UHF sensor, NBE, UHF signals, finite and small antennas.

## Article History

Article Received: 5 March 2019

Revised: 18 May 2019

Accepted: 24 September 2019

Publication: 27 December 2019

## 1. Introduction

Lightning is an electrical breakdown process and has been established that electrical breakdown is started with the very first event known as electron avalanches, followed by streamers and leaders [1, 2]. However, it is still

practically unclear about the breakdown mechanism and some researchers suggest that the frequency response of the electron avalanche peaked in ultra-high frequency (UHF) band, suggested at around 1 GHz based on numerical simulation results in Cooray and Cooray, 2012 [3]. On the other hand, others

suggest that the frequency response of the electron avalanche peaked within VHF band, which is same as the frequency response of streamers.

Electric field measurement of lightning flashes at UHF and microwave bands had been started since decades ago by implementing different types of receivers. The microwave radiation is associated primarily with the formation of streamers based on the observation results which found that both stepped leader and dart leader have strong impulsive radiation by using 0.42 and 0.85 GHz helical antennas with 1.5 MHz bandwidth [4]. UHF radiation by real lightning at Lenin Hills of Moscow during the summer of 1968 was observed by using four UHF band receivers that operated at 400, 700, 900 and 1300 MHz [5]. The lightning sensing system (include those four UHF receivers) was triggered with a frame antenna operates from 2 to 60 kHz. The measurement results of lightning radiations at 2.2 GHz from CG flashes in Florida, July 1977 by using steerable parabolic antenna was reported by Rust et al.[6]. Some return strokes had been observed being associated with the presences of microwave radiation and the observations were carried out at 0.3, 0.5 and 0.9 GHz by using dipole antennas with 360 kHz, 350 kHz and 385 kHz of each bandwidth [7].

Fourteen years later, a radiometer had been set up to measure radiation from lightning at 37.5 GHz from millimetre wave [8]. The signals analysed were limited to those with occurrence distances within 5 km as the authors would like to minimise the attenuation of the received signals. It only could be concluded that lightning flashes do emit millimetric radiation and the spectral intensity of that millimetre wave radiation is corresponding to the temperature of the antenna. The observation of microwave radiation emitted by upward

positive lighting (UPL) from the artificial triggered lighting at 2.9 GHz by using a pyramidal horn antenna was studied by Yoshida [9] while the study of microwave radiation associated with narrow bipolar event (NBE) at 2.4 GHz frequency spectrum by using a 2.4 GHz whip antenna was documented in Ahmad et al.,2013[10]. The most recent documented experimental observation about microwave radiation from –CG flash was reported whereby the author used a 1.63 GHz ceramic patch antenna with 2 MHz bandwidth to capture the microwave radiation [11].

Meanwhile, the simulations about the behavior of electron avalanche under various scenarios such as the tip of a streamer, inside the modelling of coaxial and spherical geometries had been observed and reported by Cooray and Cooray, 2012 [3]. The electric field change results were taken into the calculations of the frequency spectrum each and the authors found out that the electron avalanche emitted at peak frequency around 100 MHz under coaxial and spherical geometries. Meanwhile, the frequency spectrum of the electron avalanche at the tip of a streamer was peaked at 1 GHz although the authors found that the results were coincident similar with the experimental results reported by Kably and Chauzy, 1988 [12], where the authors carried out experiment to study about the current produced by two spherical bodies inside their lab. Hence, Cooray and Cooray [3] postulated that the calculated 1 GHz frequency spectrum by Kably and Chauzy [12] was corresponding to the discharges of electron avalanche itself. This due to the consideration of the gap between the two spherical bodies might be too short and the background potential inside the lab was not enough sustain the development of the electron avalanche into streamer which lead to the electron avalanche discharge alone.

Throughout the literature reviews, there were different kinds of antenna used as the receiver of the UHF sensors in previous studies, but the commercialized antenna with operating around 1 GHz was not available. Therefore, we decided to design a resonating antenna with its center frequency around 1 GHz to capture the emission from lightning flashes at this frequency spectrum, based on the finding reported in Cooray and Cooray, 2012 [3]. An air-gap parallel plates antenna was chosen because of its frequency independent property of the air medium [1, 2], and flame retardant-4 (FR-4) was selected as the material because of its cheaper price but same efficiency as the commercialized metal plates antenna [13, 14]. However, the resonating antenna with its finite length dimensions (A3 size) was considered large and occupied spacing. Alternatively, a small antenna was fabricated with the largest dimension was less than one tenth of the resonating antenna. The comparison between these two antennas (finite and small antenna) was carried out to distinguish the effectiveness of these two antennas in characterizing the UHF signals associated with lightning.

## 2. Methodology

The design of finite and small antenna was carried out through parametric studies in CST. Finite antenna is the antenna with its largest dimension,  $D$  must be equivalent to the corresponding wavelength, semi-wavelength or quarter-wavelength ( $\lambda$ ,  $\lambda/2$ ,  $\lambda/4$ ) of the signal it receives while Small antenna will have its largest dimension,  $D$  is very small compared to the wavelength of the signal received ( $\lambda/50 \leq D \leq \lambda/10$ ) [15]. In order to maximize the sensitivity of the capacitive antenna, one of the options is via increasing the area of the receiving plate. Based on Eq. (1) and Eq. (2), we know that the electric field change,  $E$  is proportional to the quantity of charges,  $Q$ . The

small antenna is designed with its  $D \approx \lambda/10$  to maximize the capability of the plate to store or hold the charges based on Eq. (3), where the capacitance of the antenna is proportional to its area and increment of capacitance,  $C$  will lead to the increasing of charges,  $Q$ . The fabricated antennas were then calibrated by using vector network analyser (VNA) and deployed in measurements.

$$Q = C \times V \quad (1)$$

$$V = E \times h \quad (2)$$

$$C = \epsilon (A/d) \quad (3)$$

where  $Q$  is the amount of charge,  $C$  is the capacitance of the parallel plates antenna,  $V$  is the potential different between two plates,  $E$  is the electric field,  $h$  is the height of top plate of the antenna to the ground,  $\epsilon$  is the dielectric permittivity,  $A$  is the area of the patch, and  $d$  is the separation between two plates.

## Antenna Design and Experimental Setup

In this research, two antennas (finite and small antenna) were designed and deployed as the UHF sensor for lightning remote sensing system. The finite antenna was simulated with microwave studio to find its desired resonating frequency and radiation pattern while the small antenna was simulated under Statics and Low Frequency (LF) studio to find its E-field distribution across the air gap between two plates. The schematic diagrams for the design specification of each antenna are shown in Fig. 1 until Fig. 3 while the values for each parameter labelled inside these figures are listed in Table 1. These designs were the final outcome from the ideal simulation results. The etching of the antennas would be based on these selected parameters and then used as UHF receivers.

Before the finite antenna was used as UHF receiver in lightning remote sensing system, it was calibrated by using VNA to determine its

resonant frequency and return loss,  $S_{1,1}$ . The lightning sensing system which consisted of a Fast Antenna (FA), VHF, UHF, and derivative E-field ( $dE/dt$ ) sensors, was set up as shown in Fig. 4. These signals were then sampled by a 4 channels oscilloscope (LeCroyWavesurfer 3054) at the sampling rate of 2 GS/s each channel and were saved in 5 ms time frame. These antennas were wrapped with plastic cover each to prevent the water droplets from the patch which would affect their reading values as the water droplet itself was a charge carrier [16]. The system was setup at the rooftop of Pascasiswazah Lab I, in Faculty of Electronics Engineering and Computer Engineering (FKEKK), UTeM, Duraian Tunggal, Melaka, Malaysia (2.314077° N, 102.318282° E).

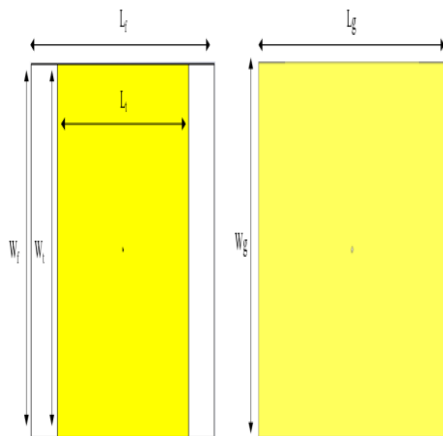


Figure 1: Top plate (left) and ground plate (right) of the antenna (yellow region is copper patch while white region is FR-4 substrate).

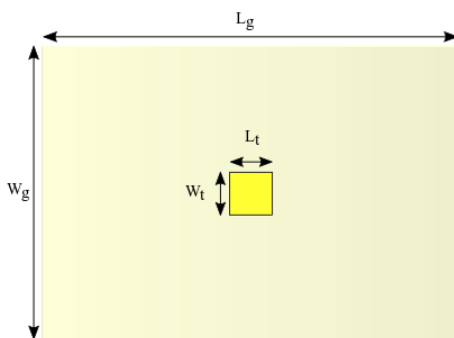


Figure 2: Schematic diagram of the small antenna (Note that the dimension of the FR-4

substrate of both top and bottom plates are equal to the dimension of the ground patch).

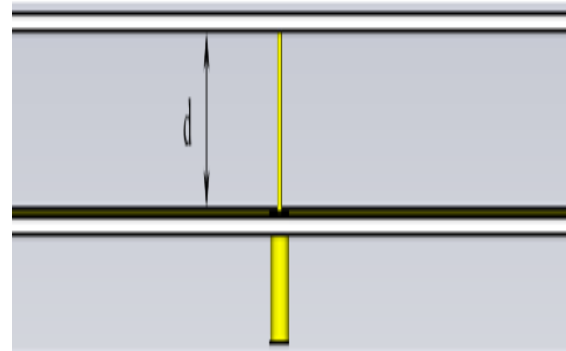


Figure 3: Separation between two plates (air gap)

Table 1: Parameters list of the finite and small antenna

Parameter	Description	Dimensions Values	
		Finite antenna	Small antenna
$L_f$	FR-4 length	420mm	297mm
$W_f$	FR-4 width	297mm	210mm
$t_f$	Thickness of FR-4	1.6mm	1.6mm
$t_{Cu}$	Thickness of copper	0.0035mm	0.0035mm
$L_t$	Top plate copper length	300mm	30mm
$W_t$	Top plate copper width	297mm	30mm
$L_g$	Bottom plate copper length	420mm	297mm
$W_g$	Bottom plate copper width	297mm	210mm
$d$	height of air gap	16mm	5mm

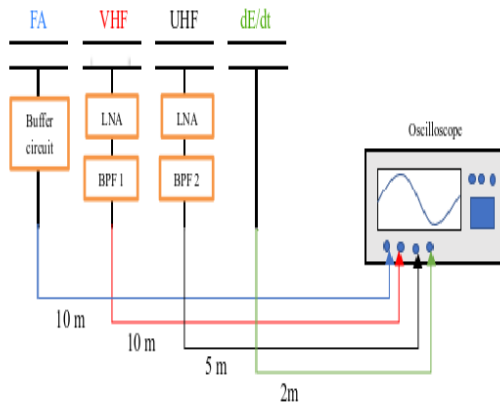


Figure 4: Schematic layout of measurement setup.

### 3. Results and Discussions

#### Antenna Simulation and Calibration

Figure 5 shows the simulated results of the finite antenna in CST. Based on Balanis, 2005[15], the largest dimension of the finite antenna,  $D$ , must be within the range of the quarter wavelength to full wavelength of the signals captured. Since we were going to capture signals at 1 GHz, the  $D$  of the antenna were set to 30 cm ( $D = \lambda$ ), and the ground area should be 60cm×60cm. However, the top patch area was adjusted to 300mm×297mm while the ground patch area turned out to be 420mm×297mm due to the limitation of the materials' dimensions were A3 size. Decreasing the dimensions of the top and ground patch would shift the resonance frequency to the left. As the result, the resonance frequency of the finite antenna varied around 0.97 GHz. The increasing of the air gap height would lead to the increasing in the return loss of the antenna together with the slightly increasing of the centre frequency. After reaching 16mm air gap, the return loss would start to decrease although the resonating frequency was still shifting towards right hand side. The simulations were done with the height of air gap varied around 15

mm due to the length of the core listed in specification was 18.7 mm. Hence, any height of the air gap larger than the actual length of the core might not be applicable.

The calibration results of the finite antenna were shown in Fig. 6. The measured return loss by using vector network analyser (VNA) was 0.97 GHz with 20 MHz bandwidth which was same as the simulation result shown in Fig. 5, although there was accompanied by another small resonating frequency. This undesired resonating frequency which was located around 3 GHz could be ignored since the antenna would be equipped with a BPF whereby the maximum pass band was 1050 MHz.

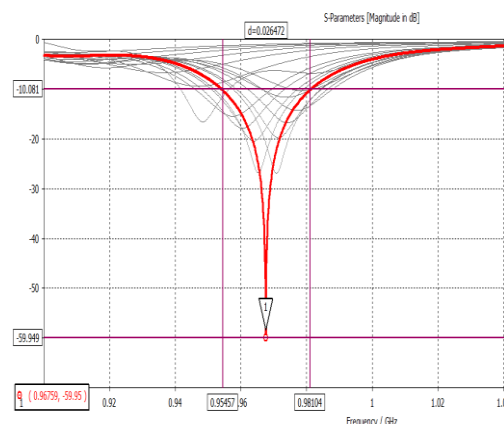


Figure 5: Return loss simulation results of the antenna from 5 mm to 20 mm air gap and the most ideal return loss was found when  $d=16$  mm.

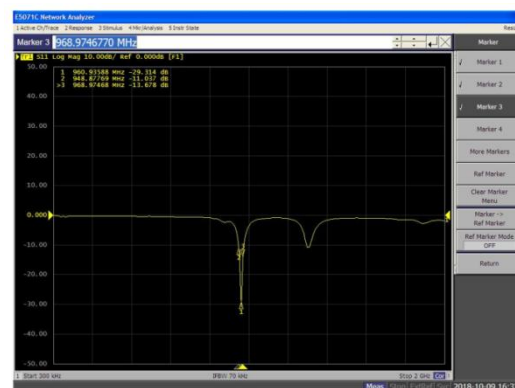


Figure 6: Return loss of the finite antenna measured by VNA.

As been stated before, the patch on top plate is maximized to 30 mm x 30 mm, which is  $\lambda/10$  of the wavelength of 1 GHz signals ( $\lambda = 0.3$  m). Therefore, the dimension of top copper patch is fixed, and the height of the air gap is manipulated from 2 mm to 30 mm. However, the larger the gap distance will lead to a greater edging effect, the detail on the observation of the electric field distribution were done at distance of air gap,  $d$  equal to 4 mm, 6 mm, 8 mm and 10 mm. Design with 2 mm gap was excluded due to the limitation of practical issue that it is difficult to create the antenna with an exact 2 mm air gap.

As shown in Fig. 7, there is no clue to prove that there is any effect of the parameter  $d$  – distance of the air gap, is proportional to the electric field change of the antenna. The simulations were run in a range of  $d$  equal to 2 mm until 30 mm with 2 mm interval each Run ID. The highest amplitude of electric field change was up to  $2.27e+015$  with 2 mm separation while the lowest e-field was  $1.105e+0.15$  with 8 mm gap. This result shows there was not much different in term of their maximum value of e-field of the antenna.

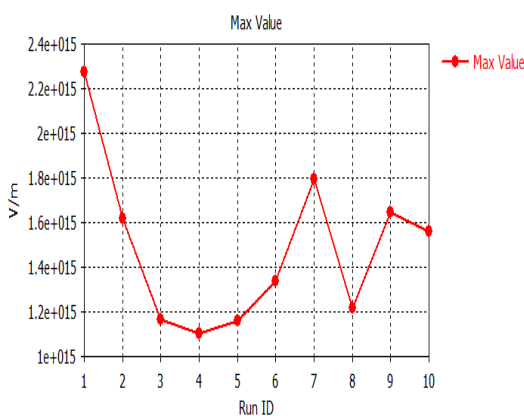


Figure 7: Maximum electric field change of the small antenna (square patch – 3mm x 3mm) across different height of the air gap (2mm until 20mm with 2mm step interval)

Figure 8 shows the electric field distribution (top view) of the antenna across different distance of the air gap. The electrical movement within or surrounding of the antenna were defined or represented by the arrows. The round-dot-liked arrows indicate that the movement of charges is perpendicular, causing them to be seemed like a perfect round dot. When the arrows start to be significantly appeared, it indicates that there is a distortion on the electric field and the charge movement tend to move in an arc manner. This phenomenon is known as edging effect or fringing effect. The ratio of the top patch was adjusted until there were 21 arrows horizontally and vertically within the top patch (example shown in Fig. 8). The red line indicates the boundary of the top patch while the purple line shows the number of lines of arrows that tend to move in such a direction that is non-perpendicular to the plates.

The simulations on this small antenna were carried out with various height of air gap (4 mm - 10 mm) to investigate the change of the edging effect of the antenna. There were only two lines of the charge movement affected by the edging effect at 4 mm air gap antenna but the number of line with non-round-dot-liked arrow increased to three lines at distance of 4 mm, 6 mm and 8 mm. 10 mm air gap antenna showed a slightly bending arrows (non-perpendicular to parallel plates) at its fourth line. This had been concluded and proven that the edging effect will significantly increase with the increasing of the parallel plates. These phenomena were due to the fringing effect itself and we could observe that this effect become severe/ greater with the increasing of the air gap height between two plates. Thus, a small antenna with 5 mm air gap was chosen to be fabricated after considering all these aspects mention above.

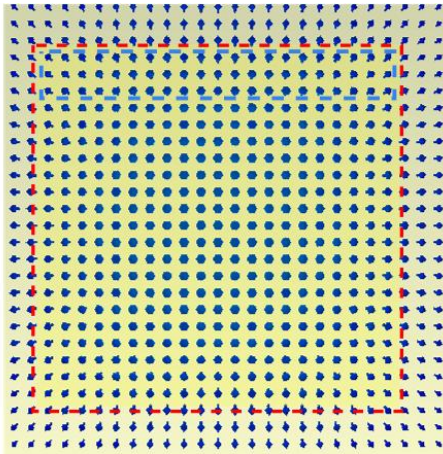


Figure 8: Edging effect when air gap was 5 mm (A4 size ground plate)

### UHF Signals Captured by the Finite Antenna and Small Antenna

Figure 9 shows the distribution of the amplitude of UHF signals by using small and finite antenna respectively. The data presented was taken during 13, 21 and 22 November 2018 by using the small antenna. The small antenna was then replaced with the finite antenna and measured the lightning signals on 4-6 and 14 December 2018. Hence, the precise comparison in term of ratio between the amplitude of each antenna could not be carried out due to the dissimilarity of the intensity of those thunderstorms (e.g. occurrence distance of lightning flashes, differences in the E-field of the source) captured by these antennas, but we could manage to compare them in term of general range of the UHF signals' amplitude as shown in that figure.

There were 120 UHF samples captured by small antenna which consisted of 144 samples of +NBEs and 6 samples of -NBEs. The maximum and minimum values of the amplitude for +NBEs was  $0.2325 \text{ V} \pm 0.0750 \text{ V}$  and  $-0.2213 \text{ V} \pm 0.0750 \text{ V}$  respectively while the maximum and minimum values of the amplitude for -NBEs was  $0.3111 \text{ V} \pm 0.1625 \text{ V}$  and  $-0.3278 \text{ V} \pm 0.1750 \text{ V}$  respectively.

On the other hand, 69 UHF samples had been captured associate with NBEs by finite antenna whereby 61 samples were +NBE while the other 8 samples were -NBE. The maximum and minimum values of the amplitude for +NBEs was  $0.3000 \text{ V} \pm 0.1376 \text{ V}$  and  $-0.2869 \text{ V} \pm 0.1125 \text{ V}$  respectively while the maximum and minimum values of the amplitude for -NBEs was  $0.2625 \text{ V} \pm 0.0688 \text{ V}$  and  $-0.2333 \text{ V} \pm 0.0438 \text{ V}$  respectively. Note that the standard deviation,  $\sigma$  was calculated based on the Eq. (4).

$$\sigma = \frac{3}{4} \times (Q_3 - Q_1) \quad (4)$$

Where  $Q_1$  was the first quartile while  $Q_3$  was the third quartile of a box plot. The result of  $Q_3$  minus  $Q_1$  was also known as interquartile range, *IQR*.

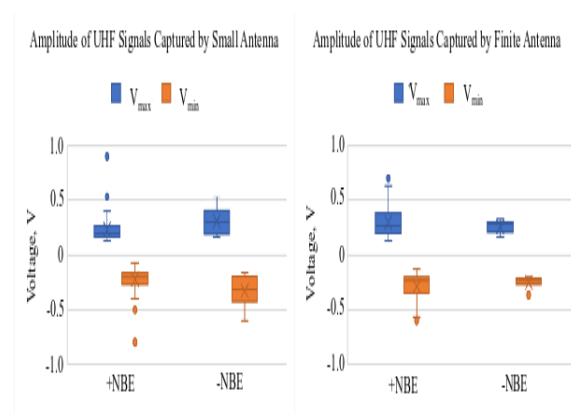


Figure 9: Statistical distribution of UHF samples' amplitude captured by small antenna and finite antenna.

Clearly, the finite antenna readings were greater than the readings of small antenna by 22.5 percent and 22.87 percent for the maximum and minimum value respectively in +NBEs. However, it was vice versa as for -NBEs whereby this phenomenon was theoretically opposite (smaller patch area should have a lower reading values) due to unknown reason. First explanation is these -NBEs (captured by the small antenna) might be

happened to be having a stronger E-field radiation than those captured by the finite antenna due to their occurrence distance were near to the base station. Perhaps the former UHF signals took place at higher altitude (region between main positive charged region and screening layer) while the latter was taking place at the lower region (e.g. region between main negative charged region and positive pocket charged region). Another explanation is the former thunderstorm was simply happened to be further away from base station compared to the latter thunderstorm. The second explanation is the former had a different breakdown mechanism that would radiate stronger emissions than the latter NBEs (captured by finite antenna).

Figure 10 and Fig. 11 gave us the visionary about the differences between the UHF signals captured by finite antenna and small antenna. These two samples with similar amplitude of their FA records were selected and compared their corresponding UHF signals to each other in Fig. 11. The Blue signal was the UHF signal captured by the finite antenna while the Red signal was the UHF signal captured by using small antenna. The Black signals were their corresponding FA records. Assuming the average noise level for both small antenna and finite antenna system were the same, the signal-to-noise ratio (SNR) of the finite antenna would be greater than small antenna, and this would improve the accuracy in characterizing the UHF signals (e.g. lower SNR would result in the condensation the UHF signals inside the noise level, making part of the signals could not be analyzed and the total pulse train duration (TPTD) of the signals would also decrease eventually). As shown in Fig. 11, the Red signal was accompanied by systematic noise and its average noise level was higher than Blue signal's. It was clearly proving that the small

antenna has a smaller SNR compared to finite antenna and the TPTD of the Red signal's burst was apparently shorter than the TPTD of Blue signal's burst.

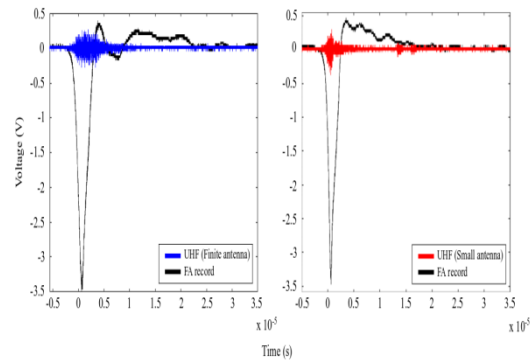


Figure 10: Examples of UHF signal (blue colour) captured by finite antenna and UHF signal (red colour) captured by small antenna. Note that the black colour signals were their corresponding +NBE (FA record).

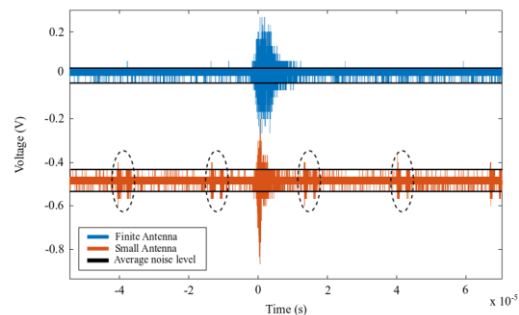


Figure 11: Comparison of UHF signals capture by finite and small antenna (UHF samples from Fig. 10). Note that the dot-circled were systematic noise picked up by the system.

#### 4. Conclusion

In conclusion, the performance of the small antenna and finite antenna in capturing the lightning signals for characterization purposes had been investigated. The finite antenna is more suitable to be deployed as UHF sensor in lightning remote sensing system due to its better sensitivity by average 20% higher than the small antenna. Further detail studies were required to determine the SNR of each antenna

precisely by implementing both antennas simultaneously, capturing and comparing the UHF signals emitted by the same source instead of considering their FA records as done in this research.

### Acknowledgements

The authors would like to acknowledge the support provided by Centre for Telecommunication Research and Innovation (CeTRI), Fakulti Kejuruteraan Elektronik dan Kejuruteraan Komputer (FKEKK), Universiti Teknikal Malaysia Melaka (UTeM) and Ministry of Education Malaysia. This project is funded by Short Term Grant (Projek Jangka Pendek PJP/2018/FKEKK/(3B)/S01615) and Fundamental Research Grant Scheme (FRGS) (FRGS/2018/FKEKK-CETRI/F00361). This research is partially funded by Universiti Teknologi Malaysia (UTM) under Q04G19 and R4F966 research grants (FRGS).

### Reference

- [1] Cooray V. An Introduction to Lightning. Dordrecht: Springer Science and Business Media; 2015.
- [2] Cooray V. Lightning Electromagnetics. United Kingdom: Institution of Engineering and Technology; 2012.
- [3] Cooray V, Cooray G. Electromagnetic radiation field of an electron avalanche. Atmospheric Research, 2012; 117: 18-27.
- [4] Brook M, Kitagawa N. Radiation from lightning discharges in the frequency range 400 to 1000 Mc/s. Journal of Geophysical Research, 1964; 69(12): 2431-2434.
- [5] Kosarev EL, Zatsepin VG, Mitrofanov AV. Ultrahigh frequency radiation from lightnings. Journal of Geophysical Research, 1970; 75(36): 7524-7530.
- [6] Rust WD, Krehbiel RR, Shlanta A. Measurements of radiation from lightning at 2200 MHz. Geophysical Research Letters, 1979; 6(2): 85-88.
- [7] Le Boulch M, Hamelin J, Weidman C. UHF-VHF Radiation from Lightning. Electromagnetics, 1987; 7(3-4): 287-331.
- [8] Fedorov VF, Frolov YA, Shishkov RO. Millimetric Electromagnetic Radiation. Journal of Applied Mechanics and Technical Physics, 2001; 42(3): 392-396.
- [9] Yoshida S. Radiations in association with lightning discharges. Japan: Department of Information and Communications Technology, Division of Electrical Electronic and Information Engineering, Graduate School of Engineering, Osaka University; 2008.
- [10] Ahmad MR, Esa MRM, Cooray V. Narrow Bipolar Pulses and Associated Microwave Radiation. In: Progress in Electromagnetics Research Symposium Proceedings, pp. 1087-1090; 2013.
- [11] Peterson D, Beasley W. Microwave radio emissions of negative cloud-to-ground lightning flashes. Atmospheric Research, 2014; 135: 314-321.
- [12] Kably K, Chauzy S. Electromagnetic radiations generated by micro discharges from hydrometeors. In: International Aerospace and Ground Conference on Lightning and Static Electricity, pp. 123-128; 1988.
- [13] Periannan D. Synthesis of capacitive and inductive antennae designed for lightning sensor application. Malaysia: Faculty of Electronics Engineering and Computer Engineering, Technical University of Malaysia Malacca; 2016.
- [14] Periannan D, Mohamad SA, Ahmad MR, Esa MRM, Sabri MHM, Seah BY, Lu G, Yusop N, Ismail MM, Abdul-Malek Z. Performance Analysis of Flame Retardant 4 Copper Plate Antenna for Lightning Remote Sensing. In: IOP Conference Series: Earth and Environmental Science, 2019; vol. 228, no. 1, p. 012006; 2019.
- [15] Balanis CA. Antenna theory: analysis and design 3<sup>rd</sup> ed. New York: John Wiley and Sons; 2005.
- [16] Seah BY, Ahmad MR, Shairi NA, Periannan D, Sabri MHM, Aziz MZAA, Ismail MM, Esa MRM, Mohammad SA, Abdul-Malek, Z, Yusop, N. The performance evaluation of capacitive antenna with various structures and permittivity values. In: 2018 International Conference on Electrical Engineering and Computer Science (ICECOS), IEEE, pp. 457-460; 2018.